Agreement Analysis and Accuracy Assessment of Multiple Mangrove Datasets in Guangxi Beibu Gulf and Guangdong-Hong Kong-Macau Greater Bay, China, for 2000–2020

Zhijie Xiao , Weiguo Jiang , Zhifeng Wu , Ziyan Ling , Yawen Deng , Ze Zhang , and Kaifeng Peng

Abstract—**Accurate and reliable mangrove datasets are essential for the protection and management of mangrove ecosystems. Therefore, the evaluation of the current mangrove datasets and understanding the differences among them are critical. This study takes the Guangxi Beibu Gulf (GBG) and Guangdong-Hong Kong-Macao Greater Bay Area (GBA) as the study areas and analyzes the agreement and accuracy of eight mangrove datasets from 2000 to 2020 using area comparison, spatial agreement analysis, and absolute accuracy evaluation. The results show that; 1) significant differences exist in mangrove area and spatial distribution among the different mangrove datasets, with the percentage of high agreement areas ranging from 10% to 42%. 2) The overall accuracy of the evaluated mangrove datasets ranges from 56.2% to 95.6%, and the classification accuracy of mangrove datasets in inland areas is lower than the overall level. 3) There are regional differences in the quality of mangrove datasets, with the agreement and accuracy of mangrove datasets in the GBG being greater than those in the GBA. 4) Fine-scale mangrove mapping based on high-resolution remote sensing images, such as Sentinel, and global mangrove mapping based on the Google Earth Engine (GEE) cloud platform should be emphasized in the future. The findings of this study can provide guidance for data users to select appropriate mangrove datasets and a reference for future mangrove mapping research.**

Index Terms—**Accuracy evaluation, Guangdong-Hong Kong-Macao Greater Bay Area (GBA), Guangxi Beibu Gulf (GBG), mangrove datasets, spatial agreement.**

I. INTRODUCTION

MANGROVES are shrubs or trees growing on tropical and subtropical coastal intertidal areas, mudflats, and riverbanks between 30° north latitude and 30° south latitude [1], [2]. Mangrove ecosystems are also one of the most productive marine ecosystems with rich biodiversity [3], [4]. Mangroves provide a variety of ecosystem services, including coastal erosion control, water purification, organic carbon fixation, habitat for animals and plants, and fisheries [5], [6], [7], [8]. However, influenced by human activities and climate change, mangroves have undergone rapid spatiotemporal changes worldwide, especially in developing regions [9]. Studies have shown that the area of mangroves in China decreased from 48 801 to 18 602 ha from 1973 to 2000, a loss rate of up to 62% [10]. Accurate and reliable mangrove datasets are crucial for the management and protection of mangrove ecosystems and can also provide data support for related research on mangroves, such as mangrove biomass estimation [11], [12].

At present, scientists have made efforts to monitor and map mangroves at local and global scales using multisource remote sensing data such as optical, hyperspectral, and radar data [2], [13], [14], [15], [16], [17], [18], [19]. The earliest mangrove datasets at a global scale were produced for the year 2000 from Global Mangrove Distribution (GMD) by Giri et al. [2] and the World Atlas of Mangroves (WAM10) by Spalding [13]. In recent years, Bunting et al. [14] used ALOS PALSAR and Landsat images to produce the mangrove dataset from the Global Mangrove Watch Project (GMW), including a new global baseline of mangrove extent for 2010 and changes from this baseline for epochs between 1996 and 2020. In 2021, Xiao et al. [15] released a 10-m resolution data product on global mangrove distribution, which is currently the highest resolution mangrove dataset at a global scale. Large areas of mangroves are distributed along the coast of China, and many studies have monitored the distribution range of mangroves in China [20], [21], [22], [23], [24], [25], [26], [27], [28], [29], [30], [31], [32]. Jia et al. [23] previously produced a 30-m resolution Chinese mangrove product for 2010 based on Landsat images. After that, Jia et al. [24] built a dataset of China's mangrove forest changes from 1973 to 2015, called the Chinese Academy of Sciences Mangroves (CAS_Mangroves). Hu et al. [26] used Landsat images to map mangroves in China from 1990 to 2015 for multiple periods. Our collaborator Peng [27] also constructed a "meta-object-knowledge" classification algorithm based on Landsat data, combining random forests and

Zhijie Xiao, Weiguo Jiang, Ziyan Ling, Yawen Deng, and Ze Zhang are with the Beijing Key Laboratory for Remote Sensing of Environment and Digital Cities, Faculty of Geographical Science, Beijing Normal University, Beijing 100875, China (e-mail: xiaozhijie@mail.bnu.edu.cn; jiangweiguo@bnu.edu.cn; lingziyan@nnnu.edu.cn; dengyawen@mail.bnu.edu.cn; zezhang@mail.bnu.edu.cn).

Zhifeng Wu is with the School of Geographical Science, Guangzhou University, Guangzhou 510006, China (e-mail: zfwu@gzhu.edu.cn).

Kaifeng Peng is with the School of Geography and Environment, Tianjin Normal University, Tianjin 300382, China (e-mail: pengkaifeng@mail.bnu.edu.cn).

hierarchical decision trees, and produced a fine category map of wetlands. Subsequent research found that China's mangroves were fragmented due to human disturbance, and it was a great challenge to accurately map Chinese mangroves using medium-resolution remote sensing images [28]. Therefore, more refined high spatial resolution remote sensing images were used to map the distribution of mangroves [28], [29], [30], [33]. For example, Zhang et al. [28] mapped the fine distribution of mangroves in China in 2018 based on 2 m resolution GF satellite images. Zhao et al. [30] produced a high-resolution mangrove map of China in 2019 based on 10 m resolution Sentinel SAR and multispectral images combined with Google Earth images. Zhang et al. [33] derived a 10-m resolution multiclass tidal wetland map of East Asia in 2020 based on Sentinel-2 images, including three types of mangroves, salt marshes, and tidal flats.

Although there are many mangrove products available, these mangrove datasets come from different organizations and researchers, and the satellite data and classification methods used are also different, which ultimately leads to differences in the accuracy and application range. Therefore, it is necessary to conduct multiscale and cross-regional comparative evaluations of some publicly available mangrove datasets, providing a reference for users to select suitable mangrove products. At present, remote sensing classification products are mainly evaluated from the two aspects of consistency and absolute accuracy, and the evaluation and analysis of multicategory land use data products is the most common [34], [35], [36], [37], [38], [39], [40], [41]. For example, Wang et al. [34] analyzed the consistency and accuracy of three land use products (i.e., FROM-GLC, ESA WorldCover, and Esri's Land Cover) in Southwest China. Liu et al. [35] evaluated the application performance of five global land cover datasets (i.e., CCI-LC, MCD12Q1, GlobeLand30, GlobCover, and CGLS-LC) in the karst region of South China from three aspects of regional comparison, spatial consistency, and precision indicators. Yang et al. [36] evaluated the similarities and differences in the area and spatial patterns of seven global land cover datasets (i.e., IGBP DISCover, UMD, GLC, MCD12Q1, GLCNMO, CCI-LC, and GlobeL30) within China. Venter et al. [40] used cross-comparison and accuracy assessment methods to evaluate three global 10 m resolution land use products from Google's Dynamic World, ESA World Cover, and Esri's Land Cover. In contrast, comparative evaluation studies on single-category remote sensing classification products, especially mangrove products, are relatively rare, which brings difficulties to the selection and use of mangrove products and greatly limits scientific research requiring mangrove maps.

The Guangxi Beibu Gulf (GBG) and Guangdong-Hong Kong-Macao Greater Bay Area (GBA) are two coastal urban agglomerations in southern China with rich and diverse wetland resources, such as mudflats, mangroves, and shallow seas [42], [43]. Since the reform and opening up, the economy in the GBA has developed rapidly. With the increase in population and the expansion of cities, the mangrove ecosystems in both areas have suffered varying degrees of damage [24]. In recent years, with the implementation of mangrove protection and restoration policies, the area of mangroves in the coastal areas of Guangxi and the Guangdong Hong Kong Macao region has significantly
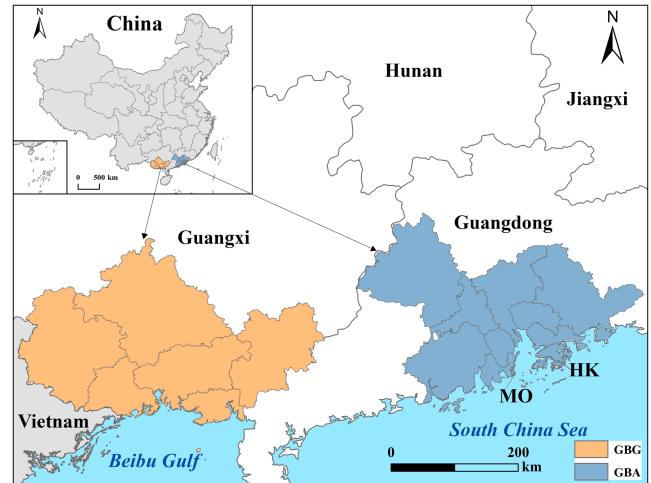

Fig. 1. Location of the study area (GBG: Guangxi Beibu Gulf; GBA: Guangdong-Hong Kong- Macao Greater Bay Area; MO: Macao; HK: Hong Kong).

increased by 2020, restoring to a historically high level [10]. Mangrove ecosystems in the two regions are closely linked to human activities, and there is a prominent conflict between people and land. The mangrove distribution has changed significantly in recent decades, making the GBG and GBA hotspots for mangrove remote sensing monitoring and related research in China [44], [45]. Therefore, a systematic assessment of the accuracy and applicability of mangrove products in the GBG and GBA is necessary to support regional scientific research, such as estimation of the carbon storage of mangroves, assessment of mangrove conservation, restoration effects, and assessment of mangrove ecological functions [46], [47].

This study selects the GBG and GBA as the study areas using the methods of area comparison, spatial pattern distribution agreement, and absolute accuracy assessment to evaluate and analyze the consistency and accuracy of various existing datasets of mangrove distributions from 2000 to 2020. In addition, factors of inconsistency are explored, and some suggestions for future mangrove mapping are given. The research results can provide a reference for future researchers to select appropriate mangrove distribution products and improve the quality of mangrove mapping in the future as well as provide necessary information for local mangrove management and protection.

II. Materials and Methods

A. Study Area

The study area of this article is the GBG and the Guangdong-Hong Kong-Macao Greater Bay Area (GBA), which are located along the southern coast of China, as shown in Fig. 1. The GBG (21° 24′ -22° 01′ N, 107° 56′ -109° 47′ E) is composed of six prefecture-level cities in the Guangxi Zhuang Autonomous Region, covering a land area of 42 500 square kilometers. Among them, Fangchenggang City, Qinzhou City, and Beihai City are adjacent to the sea, with a coastline of approximately 1595 km. GBG is located in a low-latitude zone

TABLE I
MAIN PARAMETERS OF THE EIGHT MANGROVE DATASETS ASSESSED IN THIS STUDY

| Datasets	Resolution	Time	Scale	Input data	Overall accuracy
MangroveChina_LASAC	2 m/30 m	1978-2018	China	Landsat/ZY3/GF1	>90%
Globe Mangrove Watch	30 m	1996-2020	Globe	ALOS/Landsat	95.25%
Global Mangrove Distribution	30 m	2000	Globe	GLS/Landsat	—
CAS_Mangroves	30 m	2010/2015	China	Landsat	>90%
Tidal Wetlands in East Asia	10 m	2020	East Asia	Sentinel-2	97.02%
Mangrove Map of China for 2019	10 m	2019	China	Sentinel	97%
GBG_GBA Mangrove	30 m	2000-2020	China	Landsat	—
LREIS_GlobeMangrove	10 m	2018-2020	Globe	Multisource Data	91.62%
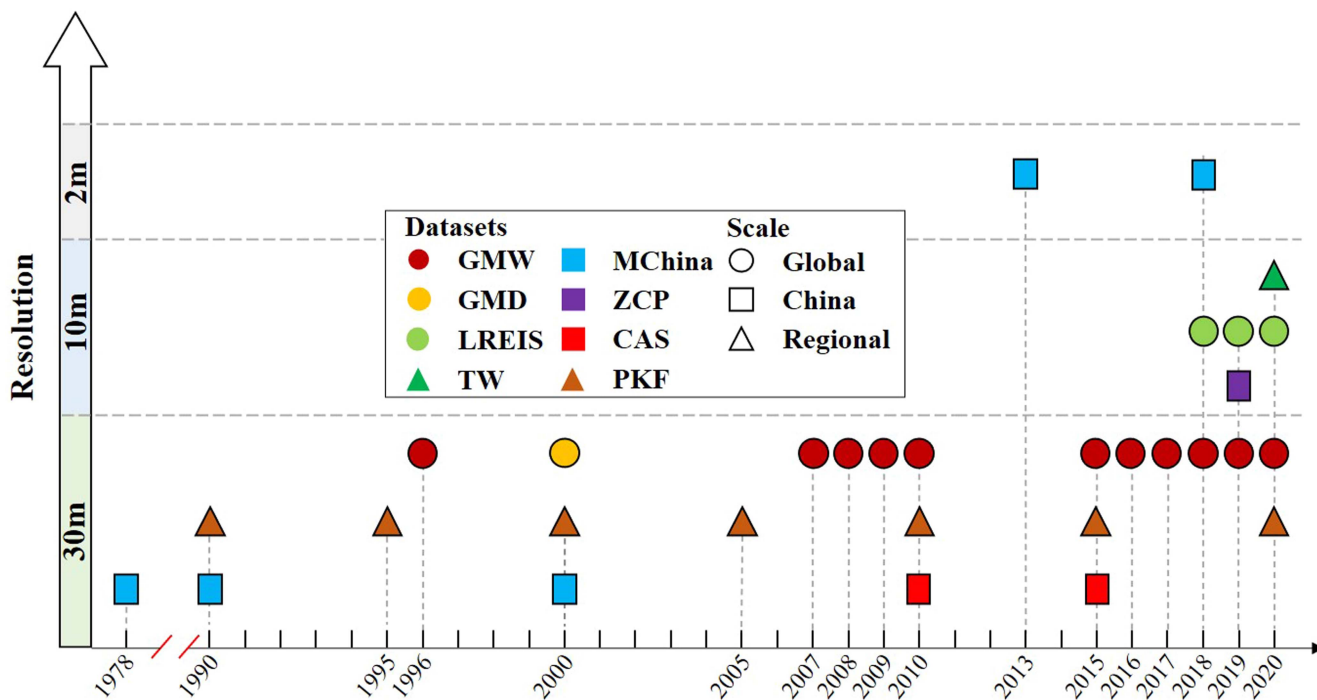
Fig. 2.   Spatiotemporal range and spatial resolution of the eight mangrove datasets assessed in this study.

and has a typical subtropical marine monsoon climate with abundant sunlight, sufficient heat, and abundant rainfall. The region is rich in wetland resources, with a large area of natural mangrove distribution. The GBA (21° 32′ - 24° 26′ N, 112° 20′ - 115° 24′ E) consists of nine prefecture-level cities in Guangdong Province and the two special administrative regions of Hong Kong and Macao, with a total area of 56 000 square kilometers. It is dominated by subtropical and tropical monsoon climate climates, with high temperatures, sufficient light, and abundant rainfall throughout the year. Mangroves, mudflats,

shallow seas, and other rich wetland resources are distributed along the 3200 km coastline of the GBA.

B. Mangrove Datasets

In this article, eight mangrove datasets were selected for accuracy and agreement analysis. Table I briefly summarizes information about these mangrove datasets, and Fig. 2 shows the spatiotemporal range and spatial resolution of the eight mangrove datasets.

MangroveChina_ LASAC (MChina) is produced by the National Land Satellite Center of the Ministry of Natural Resources of China and includes five periods of mangrove distribution data in China: 1978, 1990, 2000, 2013, and 2018. It can be accessed freely through the website (http://www.sasclouds.com/chinese/platform/newsList/notic/detail/618cc900fd423278867c5dda). The distribution of mangroves in 2018 was generated based on the 2-m resolution satellite images of ZY-3 and Gaofen-1, with an overall accuracy of 98% [28]. The distribution of mangroves in 2013 was based on the interpretation of the ZY-3 satellite images, and the distribution of mangroves in 1978, 1990, and 2000 was based on the interpretation of Landsat images, with an overall accuracy of over 90% [29].

Global Mangrove Watch (GMW) is a global mangrove dataset jointly released by Aberystwyth University (U.K.), soloEO (Japan), Wetlands International World Conservation Monitoring Centre (UNEP-WCMC), and Japan Aerospace Exploration Agency (JAXA). At present, the data are still being updated. The GMWv3 version used in this article covers the period 1996–2020, including 11 issues of mangrove distribution data, which can be accessed freely through the website (https://data.unep-wcmc.org/datasets/45). GMW used ALOS PALSAR and Landsat remote sensing images to generate a global mangrove baseline map for 2010, with an overall accuracy of 95.25%, and the remaining years' products were obtained based on changes in mangrove distribution in 2010 [14].

Global Mangrove Distribution (GMD) is a global mangrove dataset for 2000, compiled by Giri et al. [2] with funding from the United States Geological Survey (USGS) and based on Global Land Survey data and Landsat images. It can be accessed through the website (https://databasin.org/datasets/d214245ab4554bc1a1e7e7d9b45b9329/) and can also be obtained on Google Earth Engine.

CAS_Mangroves (CAS) is a mangrove spatial distribution dataset in China based on Landsat images provided by the Northeast Institute of Geography and Agroecology, Chinese Academy of Sciences Northeast Asia Resource, and Environment Big Data Center (http://www.igadc.cn/). It contains two periods of products in 2010 and 2015, and the overall classification accuracy of mangroves is more than 90%.

Tidal Wetlands in East Asia (TW) is a multiclass tidal wetland map for East Asia in 2020 produced by Zhang et al. [33] from the School of Environment and Ecology, Xiamen University, which is derived based on Sentine-2 time series images and includes three tidal wetland types: salt marshes, tidal flats, and mangroves. It can be accessed through the website(https://figshare.com/articles/dataset/Fujian_zip/14331785).

Mangrove Map of China for 2019 (ZCP) is a mangrove distribution dataset for 2019 in China produced by Zhao et al. [30] based on Sentinel satellite images with an overall classification accuracy of 97%. It can be accessed freely through the website (https://www.scidb.cn/en/detail?dataSetId = 765862389328379904&version = V1&dataSetType = personal&tag = 1&language).

GBG_GBA Mangroves (PKF) is a mangrove dataset for GBG and GBA in China produced by Peng Kaifeng, a collaborator of this study from the Department of Geographic Sciences at Beijing Normal University. The dataset covers the time range of 1990–2020 and includes seven periods of mangrove distribution products. The data are currently not publicly shared.

LREIS_ Globe Mangroves (LREIS) is a global mangrove distribution dataset for 2018–2020 produced by Xiao et al. [15], Institute of Geographic Sciences and Resources, Chinese Academy of Sciences, and other researchers based on multisource data, with an overall classification accuracy of 91.62%. It can be accessed freely through the website (https://www.scidb.cn/en/detail?dataSetId = 22b29bf879354343ba4d8d23ea0c6c66).

The above eight mangrove datasets we obtained are all vector data and unified into the WGS84 geographic coordinate system for subsequent analysis and evaluation.

C. Research Process

According to the time distribution range of the eight mangrove datasets shown in Fig. 2, mangrove products from four periods, 2018–2020, 2015, 2010, and 2000, were selected for spatial agreement and accuracy evaluation. There are six mangrove products involved in the assessment for 2018–2020 including MChina for 2018 (MChina2018), ZCP for 2019 (ZCP2019), TW for 2020 (TW2020), GMW for 2020 (GMW2020), PKF for 2020 (PKF2020), and LREIS for 2020 (LREIS2020), three for 2015, including GMW for 2015 (GMW2015), PKF for 2015 (PKF2015), and CAS for 2015 (CAS2015), three for 2010, including GMW for 2010 (GMW2010), PKF for 2010 (PKF2010), and CAS for 2010 (CAS2010), and three for 2000, including MChina for 2000 (Mchina2000), GMD for 2000 (GMW2000), and PKF for 2000 (PKF2000). Based on these mangrove products for the above four periods, an assessment is carried out of three aspects: area comparison, spatial agreement, and accuracy. The flowchart of this study is shown in Fig. 3.

D. Methodology

1) Area Comparison Analysis: The first step of our dataset comparison was to compare the mangrove area of the datasets for the four periods. Mangrove datasets were sliced from the boundary data of the GBG and GBA. To accurately calculate the area, all mangrove datasets were reprojected to the WGS84 Alberts cone projection. Area statistics for the eight mangrove datasets were conducted using ArcMap (v10.2) software to analyze the differences in mangrove distribution area in the different mangrove datasets for the same time period.

2) Spatial Agreement Analysis: To intuitively represent the spatial agreement distribution characteristics of the different mangrove datasets, this study uses spatial overlay analysis on the mangrove datasets for the periods of 2018–2020, 2015, 2010, and 2000, respectively.

The specific steps are as follows. 1) Mangrove products preparation. Mangrove products from different mangrove datasets for four periods are selected, including six mangrove products for the period of 2018–2020 and three mangrove products for each of the other three periods. 2) Overlay analysis. The spatial analysis function of ArcMap (v10.2) software is used to overlay and merge the mangrove products of the same period. 3) Spatial
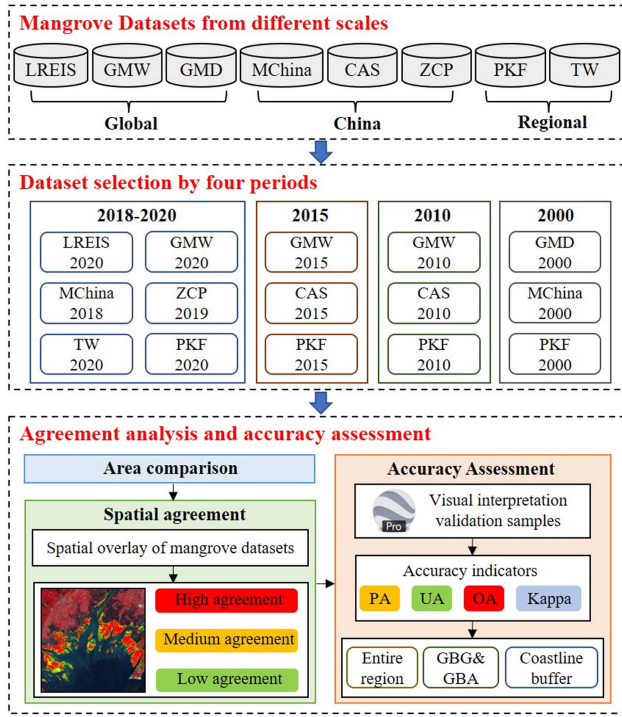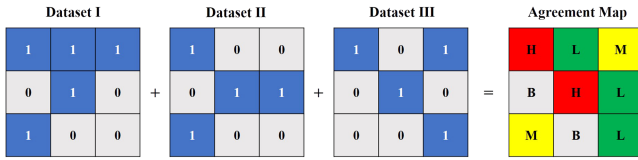
Fig. 3. Flowchart of the study.

Fig. 4. Schematic diagram of the spatial overlay process taking three datasets as an example (1: Mangrove; 0: Nonmangrove; H: High agreement; M: Medium agreement; L: Low agreement; B: Background).

agreement level division. According to the number of different mangrove products stacked together, the spatial agreement level is divided into three levels from high to low: 1) high agreement, where all three mangrove products at a certain location have mangrove distribution, or 5–6 mangrove products for the period of 2018–2020 have mangrove distribution; 2) medium agreement, where two mangrove data products at a certain location have mangrove distribution, or 3–4 mangrove products for the period of 2018–2020 have mangrove distribution; and 3) low agreement, where only one mangrove product at a certain location has mangrove distribution, or 1–2 mangrove products for the period of 2018–2020 have mangrove distribution. A schematic diagram of the spatial overlay process for mangrove datasets is shown in Fig. 4.

3) Accuracy Assessment: The confusion matrix is a commonly used accuracy assessment method to validate remote sensing classification products [48]. Based on the confusion matrix, overall accuracy (OA), producer accuracy (PA), user accuracy (UA), and kappa coefficients can be calculated to characterize the mangrove classification accuracy of each dataset.

TABLE II
NUMBER OF VALIDATION SAMPLE POINTS FOR THE FOUR RESEARCH PERIODS IN THE GBG AND GBA

Region	Type	Period			
		2020	2015	2010	2000
GBG	Mangroves	426	393	398	416
	Others	74	107	102	84
GBA	Mangroves	382	351	377	397
	Others	118	149	123	103

The calculation formulas are as follows:

$$PA = \frac{x_{ii}}{x_{+i}} \times 100\% \tag{1}$$

$$UA = \frac{x_{ii}}{x_{i+}} \times 100\% \tag{2}$$

$$OA = \frac{x_{ii}}{N} \times 100\% \tag{3}$$

$$Kappa = \frac{N \times \sum_{i=1}^{2} x_{ii} - \sum_{i=1}^{2}(x_{i+} \times x_{+i})}{N^2 - \sum_{i=1}^{r}(x_{i+} \times x_{+i})} \tag{4}$$

where x_{ii} is the correctly classified points number of type i; x_{+i} is the total points number of type i in the reference data; x_{i+} is the total points number of type i in the data to be verified; r represents the number of rows in the confusion matrix, and the value of r here is 2; N is the total number of sample points, including mangrove sample points and nonmangrove sample points.

To obtain accurate and reliable validation sample points, we mainly took the following steps: first, based on the spatial consistency results, we stratified 600 random sample points by spatial consistency level, including 300 in high consistency areas, 200 in moderate consistency areas, and 100 in low consistency areas. Then, we label 600 random points by expert visual interpretation and cross validation. Three experts label the random sample points as mangrove sample points and nonmangrove sample points by judging whether the random points are located in the mangrove area based on sentinel-2 and Google Earth high-resolution remote sensing images, and the sample points will be retained only when the three experts' judgments are consistent. Finally, for areas with sparse ground samples, we refer to the field survey data and crowdsourced data from the China Mangrove Conservation Network (CMCN, http://www.China-mangrove.org/)to supplement the sample points to ensure that the number of validation samples in GBG and GBA reaches 500 in each period. The number of validation sample points in the GBG and GBA in 2020, 2015, 2010, and 2000 is shown in Table II, and the spatial distribution of validation sample points is shown in Figs. 5 and 6. The six mangrove data products from 2018 to 2020 were evaluated for accuracy based on the validation sample points from 2020, and the mangrove data products from 2015, 2010, and 2000 were evaluated based on the corresponding year's validation sample points.
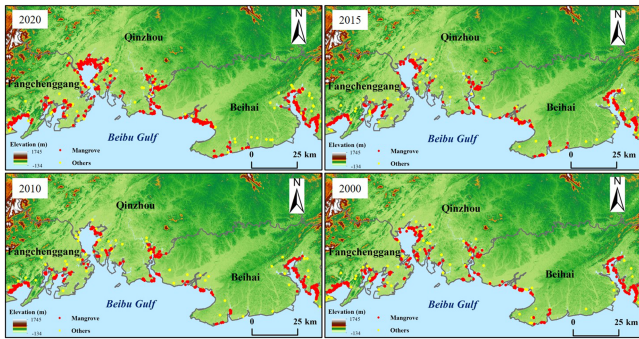
Fig. 5.   Spatial distribution of validation samples in the GBG in 2020, 2015, 2010, and 2000.
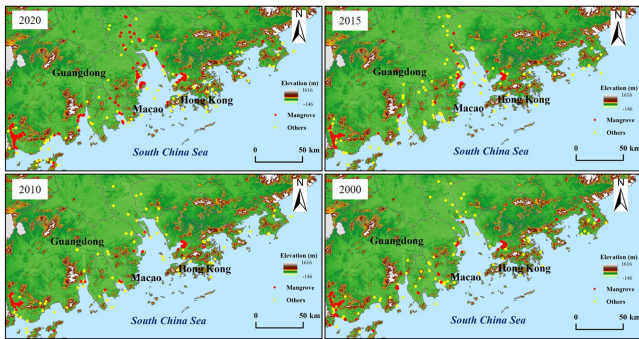

Fig. 6.   Spatial distribution of validation samples in the GBA in 2020, 2015, 2010, and 2000.

TABLE III
NUMBER OF MANGROVE VALIDATION SAMPLE POINTS AT DIFFERENT DISTANCES FROM THE COASTLINE FOR FOUR PERIODS IN THE GBG

Distance	Period			
	2020	2015	2010	2000
Inland	82	77	59	77
0–200 m	56	58	44	43
200–400 m	55	65	64	54
400–600 m	63	48	55	71
600–800 m	45	49	54	48
800–1000 m	40	28	27	43
>1000 m	85	68	93	80

To further characterize the accuracy of mangrove products with respect to distances from the coastline, taking GBG as an example, this article used the Global Self-consistent, Hierarchical, High-resolution Geography (GSHHG) coastline dataset to set up buffer zones of different distances from the coastline. These buffer zones include the inland area along the coastline, the area 0–200 m off the coastline, the area 200–400 m off the coastline, the area 400–600 m off the coastline, the area 600–800 m off the coastline, the area 800–1000 m off the coastline, and the area greater than 1 km from the coastline. The number of mangrove sample points at different distances from the coastline for four periods in the GBG is shown in Table III.

TABLE IV
AREA STATISTICS OF EIGHT MANGROVE DATASETS FOR FOUR PERIODS IN THE GBG (UNIT: HA)

Datasets	Period			
	2018–2020	2015	2010	2000
MChina	8448.95	\	\	5671.84
GMW	7839.41	8650.67	7715.66	\
GMD	\	\	\	3345.87
CAS	\	6784.56	7490.32	\
TW	7967.28	\	\	\
ZCP	8520.29	\	\	\
PKF	8164.53	6984.81	6540.85	6179.67
LREIS	8144.25	\	\	\

TABLE V
AREA STATISTICS OF EIGHT MANGROVE DATASETS FOR FOUR PERIODS IN THE GBA (UNIT: HA)

Datasets	Period			
	2018–2020	2015	2010	2000
MChina	3323.79	\	\	1312.21
GMW	1025.72	993.04	1016.43	\
GMD	\	\	\	2173.51
CAS	\	2825.84	1561.85	\
TW	2202.73	\	\	\
ZCP	3961.01	\	\	\
PKF	4091.85	3321.54	1922.67	1934.28
LREIS	4955.05	\	\	\

III. RESULT

A. Area Comparison Analysis

Tables IV and V show the area of mangrove products in the GBG and GBA, respectively, in the four periods. According to the statistical results in Table IV, the mangrove areas of the six mangrove products in the GBG during the period 2018-2020 were relatively similar. The largest area was from ZCP2019, with a total area of 8520.29 ha, and the smallest area came from GMW2020, with a total area of 7839.41 ha. In 2015, the mangrove area of GMM2015 was 8650.67 ha, which was nearly 2000 ha larger than that estimated from the CAS2015 and PKF2015 products and may have been a significant overestimation. In 2010, the mangrove areas of GMW2010 and CAS2010 were relatively similar at 7715.66 and 7490.32 ha, respectively, and the mangrove area of PKF2010 was smaller, with an area of 6540.85 ha. In 2000, the mangrove areas of MChina2000 and PKF2000 were relatively similar at 5671.84 and 6179.61 ha, respectively. The mangrove area estimated by GMD had a significant difference, with an area of only 3345.87 ha.

According to the statistical results in Table V, there were significant differences in the mangrove areas of the six mangrove products in the GBA during the period 2018–2020. The largest area was estimated by LREIS, with a total area of 4955.05 ha,
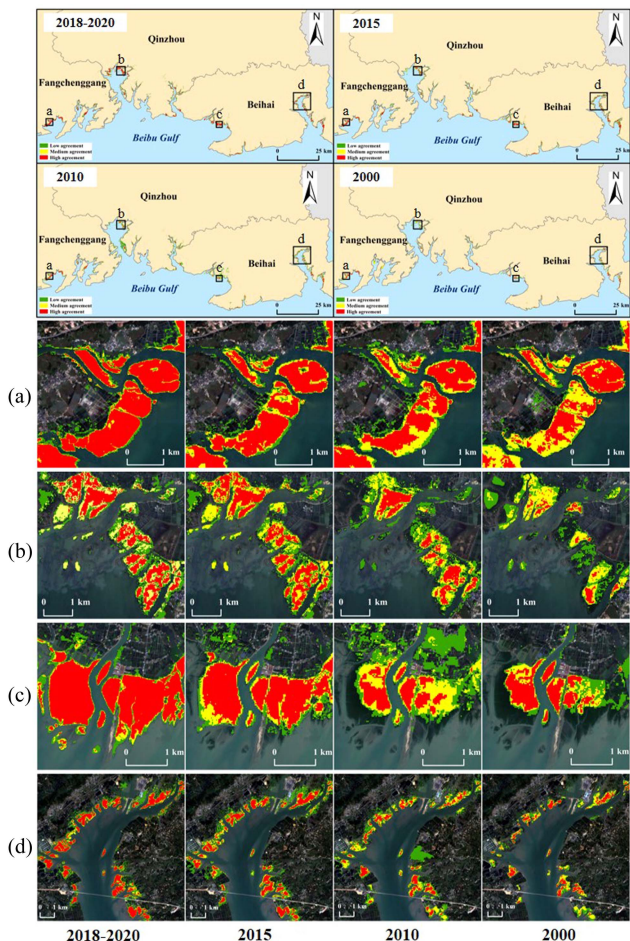
Fig. 7.   Spatial agreement distribution map of the different mangrove datasets for the four periods, 2018–2020, 2015, 2010, and 2000, in the GBG ((a), (b), (c), and (d) are four selected typical areas).
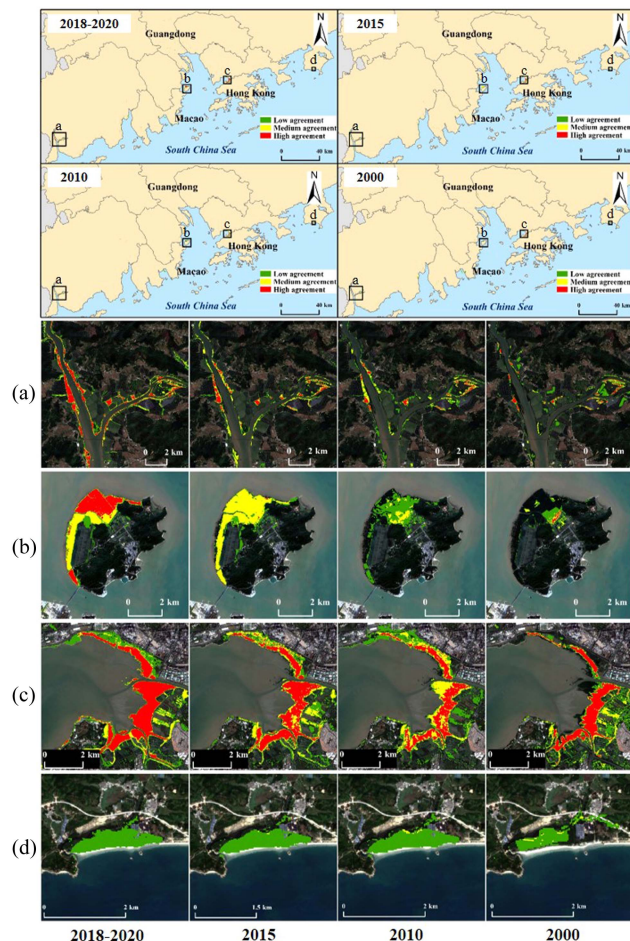

Fig. 8.   Spatial agreement distribution map of different mangrove datasets for the four periods, 2018–2020, 2015, 2010, and 2000, in the GBA ((a), (b), (c), and (d) are four selected typical areas).

while the smallest area was estimated by GMW2020, with a total area of 1025.72 ha. The average mangrove area of the six mangrove products was 3260.03 ha, and the MChina2018, ZPC, and PKF2020 products had relatively similar areas. In 2015, the mangrove area estimated by GMW2015 was 993.04 ha, which was approximately 2000 ha less than that estimated by CAS2015 and PKF2015, indicating significant underestimation. In 2010, the mangrove areas of CAS2010 and PKF2010 were relatively similar at 1561.85 and 1922.67 ha, respectively. The mangrove area estimated by GMW2010 was still smaller, with an area of 1016.43 ha. In 2000, the mangrove areas of GMD and PKF2000 were relatively similar at 2173.51 and 1934.28 ha, respectively. The mangrove area estimated by MChina2000 was smaller at 1312.21 ha.

B. Spatial Agreement Analysis

According to the spatial overlay method, the spatial agreement distribution maps of mangrove products were obtained in the GBG and GBA for the four periods, 2018–2020, 2015, 2010, and 2000, as shown in Figs. 7 and 8. Selecting typical areas for zooming in shows that the high agreement areas are mainly

distributed in the central regions of large mangrove patches, while the low agreement areas are mainly distributed in small mangrove patches or the edges of large mangrove patches. Visually comparing the spatial agreement maps of the two regions shows that the agreement of mangrove datasets in the GBG is better than that in the GBA due to the greater concentration and larger patch size of mangroves in the former and the scattered and fragmented distribution of mangroves in the latter. Furthermore, the comparison of the spatial agreement distribution maps of the four periods in the same region shows that the agreement of the earlier mangrove datasets was lower, and as time passed, the agreement among the mangrove datasets continued to improve.

Further statistical analyses were conducted on the areas of different degrees of agreement and the proportions of high agreement regions for the four periods in the GBG and GBA, as shown in Fig. 9. The area of the low agreement was the highest in the GBG and GBA for the four periods, and the area of low agreement in the GBA exceeded the sum of the areas of the high and medium agreement. The statistical results also showed that the agreement of mangrove products in the GBG was better than that in the GBA, with high agreement regions accounting for over 20% for all four periods in the GBG, while in the GBA,
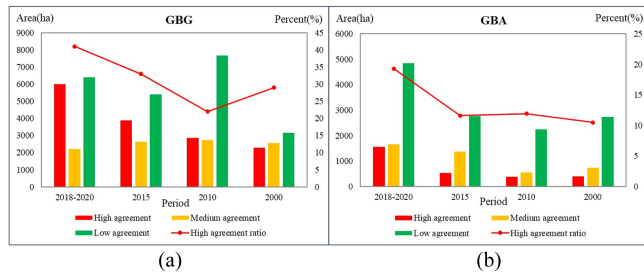
Fig. 9. Spatial agreement area statistic and high agreement area ratio during the four periods in the GBG and GBA.
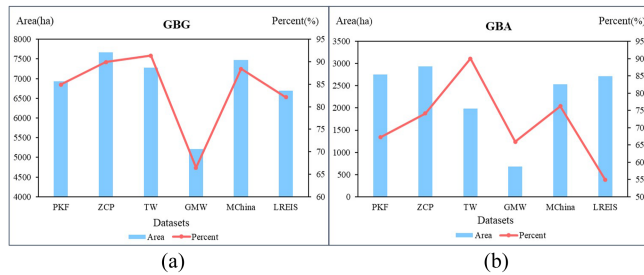

Fig. 10. Area and ratio statistics of the medium and high agreement regions for the six mangrove datasets assessed during the period 2018–2000 in the GBG and GBA.

the proportion of high agreement regions for the four periods was less than 20%.

To further quantify the contributions of the different mangrove products to the spatial agreement, using 2018–2020 as an example, the areas of high and medium agreement belonging to each mangrove product and their proportion to the total area of the product's mangrove distribution range were calculated, as shown in Fig. 10. According to the statistical results for GBG [see Fig. 10(a)], ZCP and MChina2018 had the largest areas at 7662.19 and 7468.47 ha, respectively, and TW and ZCP had the largest proportions, accounting for 91.37% and 89.93%, respectively. The product with the smallest area and proportion was GMW2020, which had only 5209.88 ha of mangroves in the high and medium agreement regions, accounting for 66.46% of the total area of the product's mangrove distribution range. In addition, based on the statistical results for the GBA [see Fig. 10(b)], ZCP and PKF2020 had the largest areas at 2936.19 and 2750.20 ha, respectively, and TW2020 and MChina2018 had the largest proportions, accounting for 90.00% and 76.24%, respectively. The product with the smallest area was GMW2020, with only 676.45 ha, and the proportion of the smallest area was LREIS, accounting for 54.86%. Therefore, three data products, ZCP2019, MChina2018, and TW2020, can be considered to have performed well in terms of spatial agreement, while GMW2020 and LREIS showed significant differences from the other mangrove products.

C. Accuracy Evaluation

1) Overall Accuracy Analysis in the Entire Study Area:
In general, the overall accuracy of the eight mangrove datasets in
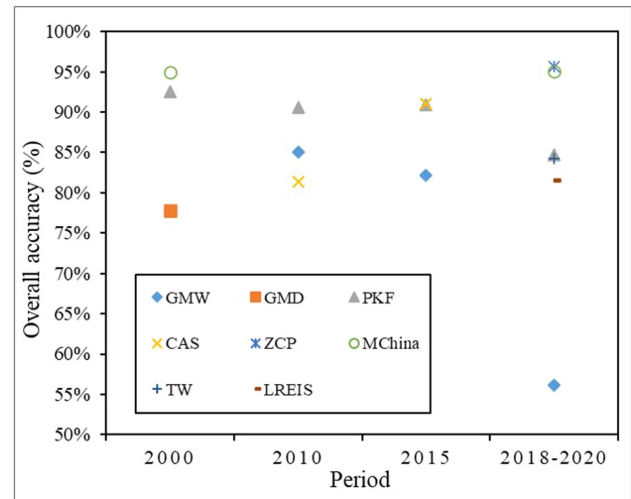

Fig. 11. Overall accuracy of the eight mangrove datasets in the entire study area for 2000–2020.

the four periods of the entire study area ranges from 56.2% to 95.6% and presents a distinctive pattern as shown in Fig. 11. In 2018–2020, ZCP (95.6%)>MChina2018 (95.1%)>PKF2020 (84.7%)> TW (84.3%)> LREIS (81.6%)>GMW2020 (56.2%); in 2015, CAS (91.0%)>PKF (90.9%)>GMW (82.2%); in 2010, PKF2010 (90.6%)>GMW2010 (85.1%)>CAS2010 (81.4%); and in 2000, MChina2000 (94.9%)> PKF2000 (92.5%)>GMD (77.8%). Therefore, the accuracy of the national- or regional-scale mangrove datasets in the study area is higher than that of the global-scale mangrove datasets. In addition, mangrove data products that use high-resolution remote sensing imagery as the classification data source perform extremely well, such as MChina2018, based on GF high-resolution images with a resolution of 2 m, and ZCP, based on Sentinel images with a resolution of 10 m, which both exhibit the highest accuracy.

2) Accuracy Evaluation for GBG and GBA:
The overall accuracy and kappa coefficient of the mangrove datasets in the four periods in the GBG are shown in Table VI. For 2018–2020, ZCP and MChina2018 have the highest accuracy; GMW2020 and LREIS have the lowest accuracy. In 2015, the accuracy of CAS2015 was the highest, while GMW had the lowest accuracy. In 2010, PKF2010 had the highest accuracy, while CAS2010 had the lowest accuracy. In 2000, MChina2000 had the highest accuracy, and GMD had the lowest accuracy.

From the perspective of producer accuracy and user accuracy (see Fig. 12), the producer accuracy of the different mangrove datasets in the GBG varies significantly among the same periods. Among the six mangrove products evaluated in the 2018–2020 period, ZCP had the highest producer accuracy of 96.5%, while GMW had the lowest producer accuracy of only 59.4%. In 2015, the producer accuracy of the three data products was between 88.3% and 92.6%. Similarly, in 2010, the producer accuracy of the three data products was between 86.7% and 93.2%. In 2000, the producer accuracy of the three data products was between 76.7% and 94.5%. In comparison, the user accuracy of the mangrove datasets in the different periods is always high and

TABLE VI
OVERALL ACCURACY AND KAPPA COEFFICIENT OF THE MANGROVE DATASETS
FOR THE FOUR PERIODS IN THE GBG

Period	Dataset	Precision (%)	
		OA	Kappa
2018–2020	MChina	96.4	86.9
	GMW	63.4	24.0
	TW	86.8	60.5
	ZCP	96.8	88.2
	PKF	84.6	54.8
	LREIS	83.2	53.6
2015	GMW	82.6	49.1
	PKF	92.6	79.5
	CAS	93.8	82.5
2010	GMW	82.4	46.2
	PKF	87.6	60.7
	CAS	81.2	44.5
2000	MChina	94.2	80.8
	PKF	89.8	61.2
	GMD	76.2	37.2

TABLE VII
OVERALL ACCURACY AND KAPPA COEFFICIENT OF THE MANGROVE DATASETS
FOR THE FOUR PERIODS IN THE GBA

Period	Dataset	Precision (%)	
		OA	Kappa
2018–2020	MChina	93.8	83.8
	GMW	49.0	17.7
	TW	81.8	59.6
	ZCP	94.4	84.2
	PKF	84.8	60.2
	LREIS	80.1	45.8
2015	GMW	81.8	60.0
	PKF	89.2	71.6
	CAS	88.2	69.0
2010	GMW	87.8	69.4
	PKF	93.6	82.6
	CAS	81.6	49.9
2000	MChina	95.6	87.2
	PKF	95.2	85.0
	GMD	79.4	44.4

Fig. 12. Producer accuracy (a) and user accuracy (b) of the eight mangrove datasets during the four periods in the GBG.
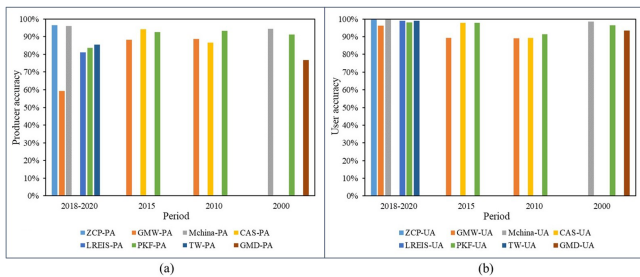

Fig. 13. Producer accuracy (a) and user accuracy (b) of the eight mangrove datasets for the four periods in the GBA.

relatively similar. In the 2018–2020 period, the user accuracy of all six data products exceeded 96%. In 2015, the user accuracy of the three data products was between 89.4% and 97.9%. In 2010, the user accuracy of the three data products was between 89.1% and 91.4%. In addition, in 2000, the user accuracy of the three data products was between 93.5% and 98.5%.

The overall accuracy and kappa coefficient of the mangrove datasets in the different periods of the GBA are shown in Table VII. The results show that for 2018–2020, ZCP and MChina2018 had the highest accuracy; GMW2020 and LREIS had the lowest accuracy. In 2015, the accuracy of PKF2015 was the highest. In 2010, PKF2010 had the highest accuracy; CAS2010 had the lowest accuracy. In 2000, the accuracy of MChina2000 was the highest; the accuracy of GMD was the lowest.

In terms of producer accuracy and user accuracy (as shown in Fig. 13), there are significant differences in the producer accuracy of the mangrove datasets in the GBA during the four periods. Among the six datasets evaluated during 2018–2020, ZCP had the highest producer accuracy of 97.1%, while GMW
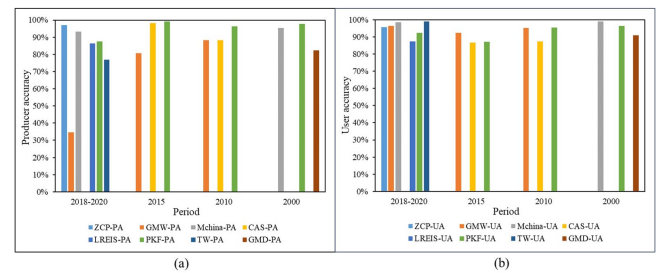
had the lowest producer accuracy of only 34.6%. In 2015, the producer accuracy of the three datasets ranged between 80.6% and 99.1%. In 2010, the producer accuracy of the three datasets ranged between 88.3% and 96.2%. In addition, in 2000, the producer accuracy of the three datasets ranged between 82.5% and 97.7%. For user accuracy, mangrove datasets for the four periods in the GBA all had accuracies of over 85%. During 2018–2020, the user accuracy of the six datasets ranged between 87.4% and 99%. In 2015, the user accuracy of the three datasets ranged between 86.7% and 92.4%. In 2010, the user accuracy of the three datasets ranged between 87.4% and 95.1%. In addition, in 2000, the user accuracy of the three datasets ranged between 90.8% and 99.0%.

Comparing the accuracy evaluation results of the mangrove datasets in the GBG and the GBA, the accuracy of the same mangrove product in the GBG is higher than that in the GBA. Taking the period 2018–2020 as an example, in the GBG, the overall accuracy is higher than 4.5% on average, and the kappa coefficient is 2.8% higher on average, indicating that the heterogeneity of mangrove distribution in different regions can have a clear impact on the mangrove classification accuracy.
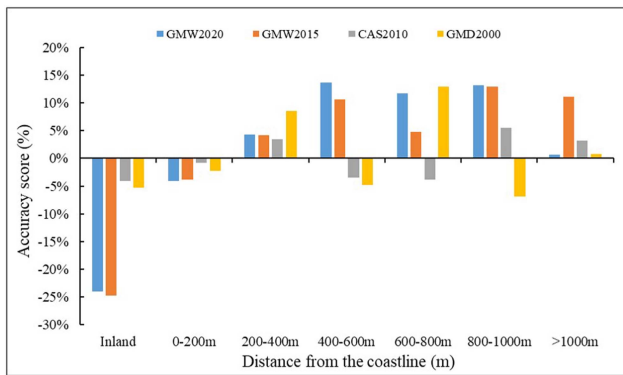
Fig. 14. Accuracy score of four mangrove products at different distances from the coastline.

3) Accuracy Evaluation at Different Distances From the Coastline: Based on mangrove sample points at different distances from the coastline (as shown in Table III), the classification accuracy of the lowest accuracy mangrove products in the four periods in the GBG was evaluated, attempting to find the reasons for the low accuracy of these mangrove products. To highlight the contrast effect, the accuracy scores obtained by subtracting the producer accuracy of mangrove data products in each buffer area from the producer accuracy of the product in the overall area are shown in Fig. 14. The accuracy scores of the four data products in the inland area and the 0–200 m coastal buffer zone were all lower than 0, and the accuracy scores of GMW2020 and GMW2015 were nearly −25% in the inland area, indicating that the classification accuracy of mangroves is poor in near land areas. However, in areas more than 200 m off the coastline, most of the accuracy scores of the mangrove products were higher than 0, indicating that the overall accuracy of the mangrove classification is better in offshore areas. The reason for this may be that other evergreen vegetation growing in nearshore areas is easily confused with mangroves, which brings challenges to the accuracy of mangrove mapping.

IV. DISCUSSION

A. Comprehensive Evaluation

This study systematically evaluated the available mangrove datasets from 2000 to 2020 in the GBG and the GBA in terms of area comparison, spatial agreement, and absolute accuracy. For the area comparison, global-scale mangrove datasets such as GMW and GMD have obvious differences in area from the other mangrove data products for the same period.Regarding spatial agreement, among the evaluated mangrove products for 2018–2020, TW, ZCP, and MChina showed higher spatial agreement with other mangrove data products, while GMW and LREIS showed lower spatial agreement. For the accuracy evaluation, the differences in producer accuracy among the four periods of mangrove data products were significant, while the differences in user accuracy were relatively low. This indicates that misclassifying nonmangrove areas as mangrove areas was rare in all mangrove datasets, and the differences in classification

accuracy were reflected in the completeness of the extracted mangrove distribution ranges. During the period 2018–2020, the overall accuracy of ZCP and MChina was the highest, at 95.6% and 95.1%, respectively, while the overall accuracy of GMW was the lowest, at only 56.2%. In 2015, the overall accuracy of CAS was the highest, at 91%, while that of GMW was the lowest, at only 82.2%. In 2010, the overall accuracy of PKF was the highest, at 90.6%, while that of CAS was the lowest, at only 81.4%. In 2000, the overall accuracy of MChina was the highest, at 94.9%, while that of GMD was the lowest, at only 78.8%. Based on the above evaluation analysis, for further research on mangroves in the GBG and GBA, the MChina and ZCP datasets should be preferentially selected as the basic data for mangrove distribution. For specific years, the use of CAS datasets is recommended for 2015, and the use of PKF datasets is recommended as a supplement for 2010.

In conclusion, different mangrove datasets have their own advantages and disadvantages. Among them, GMD, GMW, and LREIS, as global mangrove datasets, are of great significance for understanding the distribution of global mangroves, but there is still room for improvement in accuracy. In particular, GMD, as an early mangrove dataset, provides ideas and method guidance for subsequent mangrove mapping research. The time range of the GMW dataset covers 1996–2020, which has a good reference value for understanding the dynamic changes of mangroves around the world. As a global mangrove dataset, LREIS's overall accuracy in the GBG and the GBA is close to that of small-scale mangrove datasets of the same period, and has great application potential. The PKF dataset covers a wide time range, but its spatial range only includes GBG and GBA. MChina, ZCP, and CAS, as three China-wide mangrove datasets, provide valuable data for mangrove-related research in China. Among them, the MChina dataset used GF images as the data source in 2013 and 2018 to achieve remote sensing monitoring of mangroves with a resolution of 2 m, and obtained a precise and accurate distribution of mangroves in China. The ZCP dataset uses free Sentinel images as the data source to achieve methodological and theoretical innovation, and the classification obtains the distribution of mangroves in China with a high-precision 10m resolution. The CAS dataset is an earlier China-wide mangrove dataset with 30m resolution. It also has good data accuracy and fills the gaps in China's mangrove distribution data in 2010 and 2015. The TW dataset covers the entire East Asia region and has high spatial resolution and data accuracy. The dataset not only includes mangrove categories but also salt marsh and tidal flat categories, and is of unique value for studying mangrove wetland ecosystems.

B. Factors of Differences Among the Mangrove Products

The analysis of the agreement and accuracy of various mangrove datasets from 2000 to 2020 shows certain differences among different mangrove datasets. This study suggests that the main reasons for the differences are as follows.

1) The difference in the classification spatial scale directly affects the consistency among the datasets. The GMW, GMD, and LREIS mangrove datasets at the global scale

have lower agreement and classification accuracy than other mangrove datasets at the national and regional scales. This is related to the difficulty of mangrove classification at the global scale, such as the selection of accurate samples and the differences in mangrove species and characteristics in different regions, which easily lead to deviations between global mangrove datasets and the actual distribution of mangroves in specific locations [2]. In contrast, global mangrove mapping requires significant time and cost, and thus, to avoid redundant classification processes, some long-term mangrove datasets will use the mangrove distribution of a specific year as a baseline, and the mangrove distribution of other years will be corrected accordingly. However, mangrove ecosystems are significantly affected by human activities and tidal changes, and their distribution ranges change over time, leading to a decrease in accuracy for nonbaseline year mangrove products [49]. For example, the GMW dataset used the product for 2010 as the baseline, and its classification accuracy of the mangrove map for 2010 was significantly higher than that for other years.

2) The difference in data sources is also the main factor leading to inconsistencies. The resolution of the data source directly affects the accuracy of classification, especially in the mangrove boundary areas, where inconsistencies are particularly evident. Data source with higher resolution can extract mangrove boundaries more precisely and effectively reduce interference from mixed pixels [50], [51]. For example, PKF2020 uses Landsat 30 m resolution remote sensing images as its data source, and its classification accuracy is significantly lower than that of MChina2018 using 2 m high-resolution images from the GF satellite as the data source and ZCP using Sentinel-2 10-m resolution remote sensing images as the data source.

3) Different classification methods and strategies can also affect the consistency between different datasets. At present, most mangrove products are classified using machine learning methods such as random forest classifiers and support vector machines, but there are also differences in classification strategies such as feature selection, image selection and processing, sample point selection, and postclassification processing. For example, ZCP uses multisource and multitemporal classification features [52], TW integrates tidal and phenological features [33], CAS adopts object-oriented methods [23], and MChina uses meticulous manual editing and strict on-site verification of classification results in postprocessing [28]. These methods and strategies have improved the accuracy of mangrove classification to varying degrees, but also caused differences between mangrove datasets.

4) Tidal inundation affects consistency between mangrove datasets. Mangroves grow in the intertidal zone of the coast, and some mangrove areas are regularly submerged by tides. Therefore, only when the remote sensing image is captured at the lowest tide level and the mangrove is completely exposed on the mudflat, a complete mangrove mapping result can be obtained. However, in most cases, the images available for mapping are not recorded at the lowest tide level, and may even be obtained at high tide level, leading to an underestimation of the spatial distribution of mangroves. So even for mangrove datasets of the same year, differences in the acquisition time of the original images used can lead to variations in the degree of tidal inundation affecting the mangroves, ultimately resulting in inconsistency among the mangrove datasets [53], [54], [55]. This study only compares the consistency of mangrove spatial distribution from various mangrove datasets to identify more applicable mangrove products. Subsequent research will quantitatively explore the impact of tidal inundation on mangrove spatial distribution.

5) Moreover, the number and quality of validation samples can also impact the results of the consistency evaluation. The validation sample points used in this study were mainly selected through visual interpretation of Google Earth images and may be conservative due to personal subjective factors in the selection of sample points. In particular, for nonmangrove sample points, only points determined not to be mangrove areas were selected, which may be the reason for the high user accuracy of various mangrove data products. Therefore, it is essential to establish a shared and updated mangrove sample library for the production of mangrove products and analysis of their results [56].

C. Implications for Future Mangrove Mapping

For future research on mangrove mapping, the results of this study primarily suggest the following three points.

1) First, mangroves should be mapped at fine resolution. The European Sentinel-2A and Sentinel-2B satellites, launched by the European Space Agency in June 2015 and March 2016, respectively, can provide global coverage with 5 day repeat and 10 m spatial resolution imagery. Their data are publicly available and can be used to conduct high-temporal and spatial monitoring of mangroves [57]. In addition, the analysis results of this study show that the use of high-resolution remote sensing images can enhance the identification of small and fragmented mangrove areas, thereby improving the accuracy of mangrove classification results. Therefore, the use of high-resolution remote sensing imagery for fine-resolution mangrove mapping is recommended.

2) Second, mangroves should be mapped on a global scale. According to the results of this study, the existing global-scale mangrove products, such as GMW and GMD, still have room for improvement in accuracy. Meanwhile, the new cloud computing platform Google Earth Engine (GEE) can access large amounts of remote sensing data, and its powerful processing capabilities also provide great convenience for the production of global-scale data products [58], [59]. Therefore, the use of the GEE cloud platform to perform global-scale mangrove mapping in the future is recommended.

3) Finally, conducting mangrove mapping research by integrating multisource data is recommended [60], [61]. Based on the research results, the classification accuracy of mangrove data products in inland areas is lower than the overall level. This may be due to the high spectral similarity between mangroves and terrestrial vegetation, which can easily lead to confusion and misclassification [62]. Therefore, the use of multispectral and hyperspectral data fusion and multisensor data fusion shows enormous potential for future mangrove mapping. For example, during the production process of the ZCP product, Sentinel-1 SAR images, Sentinel-2 optical images, and digital terrain data were used to classify mangroves, effectively improving the accuracy of mangrove classification.

V. CONCLUSION

This article takes the GBG and GBA as the study areas and uses methods such as area comparison, spatial agreement, and accuracy assessment to analyze the consistency of various mangrove distribution datasets in four periods, 2018–2020, 2015, 2010, and 2000. Eight mangrove datasets were evaluated: MChina, ZCP, TW, GMW, LREIS, PKF, CAS, and GMD. The main conclusions of the study are as follows.

1) From the results of the area comparison and spatial agreement analysis, significant differences exist in mangrove area and spatial distribution among the different mangrove datasets in the study area. The percentage of high agreement areas in the four periods is between 10% and 42%.

2) From the results of the accuracy evaluation, the overall accuracy of the evaluated mangrove datasets is between 56.2% and 95.6%. The ZCP and MChina datasets have the highest accuracy at approximately 95%, and the GMW dataset has the lowest accuracy, between 56.2% and 85.1%. In addition, due to the influence of other land-based evergreen vegetation, the classification accuracy of mangrove datasets in inland areas is lower than the overall level.

3) From the perspective of regional comparison, the agreement and accuracy of mangrove datasets in the GBG are better than those in the GBA. The percentage of high agreement areas is higher by 10%–20%, the overall accuracy in the 2018–2020 period is on average 4.5% higher, and the kappa coefficient is on average 2.8% higher. The mangroves in the GBA are more closely related to human activities. They are scattered and fragmented, which poses greater challenges to mangrove mapping.

4) For future mangrove mapping, from the perspective of spatial resolution, the 30-m resolution mangrove dataset has a more complete time range, but its accuracy is limited. The higher resolution mangrove datasets produced based on Sentinel, GF, and other satellite images have sufficient accuracy, but they are only single-period data for each year. Therefore, long-time sequence fine-scale mangrove mapping should be based on high-resolution remote sensing satellite images such as Sentinel to meet the needs of precise and continuous mangrove monitoring

in the future. From the classification scale perspective, the accuracy of the global mangrove dataset still has room for improvement. The rise of the computer cloud platform GEE has brought great convenience for global mangrove mapping. Utilizing the GEE cloud platform to carry out global-scale mangrove mapping has tremendous application potential.

In general, the findings of this study not only provide guidance for data users to select appropriate mangrove datasets but also provide some reference for future mangrove mapping research. At the same time, this study also provides necessary information for remote sensing monitoring and conservation management of mangroves in the GBG and GBA.

REFERENCES

[1] C. D. Field, "Rehabilitation of mangrove ecosystems: An overview," *Mar. Pollut. Bull.*, vol. 37, no. 8–12, pp. 383–392, 1999.

[2] C. Giri et al., "Status and distribution of mangrove forests of the world using earth observation satellite data," *Glob. Ecol. Biogeography*, vol. 20, no. 1, pp. 154–159, 2011.

[3] D. M. Alongi, "Present state and future of the world's mangrove forests," *Environ. Conservation*, vol. 29, no. 3, pp. 331–349, 2002.

[4] P. J. Mumby et al., "Mangroves enhance the biomass of coral reef fish communities in the Caribbean," *Nature*, vol. 427, no. 6974, pp. 533–536, 2004.

[5] B. K. Veettil, S. F. R. Pereira, and N. X. Quang, "Rapidly diminishing mangrove forests in Myanmar (Burma): A review," *Hydrobiologia*, vol. 822, pp. 19–35, 2018.

[6] S. Das and A.-S. Crépin, "Mangroves can provide protection against wind damage during storms," *Estuarine, Coastal Shelf Sci.*, vol. 134, pp. 98–107, 2013.

[7] D. C. Donato, J. B. Kauffman, D. Murdiyarso, S. Kurnianto, M. Stidham, and M. Kanninen, "Mangroves among the most carbon-rich forests in the tropics," *Nature Geosci.*, vol. 4, pp. 293–297, 2011.

[8] E. B. Barbier, S. D. Hacker, C. Kennedy, E. W. Koch, A. C. Stier, and B. R. Silliman, "The value of estuarine and coastal ecosystem services," *Ecological Monographs*, vol. 81, no. 2, pp. 169–193, 2011.

[9] M. S. Li, L. J. Mao, W. J. Shen, S. Q. Liu, and A. S. Wei, "Change and fragmentation trends of Zhanjiang mangrove forests in southern China using multi-temporal Landsat imagery (1977–2010)," *Estuarine, Coastal Shelf Sci.*, vol. 130, pp. 111–120, 2013.

[10] M. Jia, Z. Wang, D. Mao, C. Huang, and C. Lu, "Spatial-temporal changes of China's mangrove forests over the past 50 years: An analysis towards the sustainable development goals (SDGs)," *Chin. Sci. Bull.*, vol. 66, pp. 3886–3901, 2021.

[11] L. T. Pham and L. Brabyn, "Monitoring mangrove biomass change in Vietnam using SPOT images and an object-based approach combined with machine learning algorithms," *Int. Soc. Photogrammetry Remote Sens. J. Photogrammetry Remote Sens.*, vol. 128, pp. 86–97, 2017.

[12] J. A. A. Castillo, A. A. Apan, T. N. Maraseni, and S. G. Salmo III, "Estimation and mapping of above-ground biomass of mangrove forests and their replacement land uses in the Philippines using Sentinel imagery," *Int. Soc. Photogrammetry Remote Sens. J. Photogrammetry Remote Sens.*, vol. 134, pp. 70–85, 2017.

[13] M. Spalding, *World Atlas of Mangroves*. England, U.K.: Routledge, 2010.

[14] P. Bunting et al., "The global mangrove watch—A new 2010 global baseline of mangrove extent," *Remote Sens.*, vol. 10, no. 10, 2018, Art. no. 1669.

[15] H. Xiao et al., "10-m global mangrove classification products of 2018-2020 based on big data," *Sci. Data Bank*, 2021.

[16] Y. Zheng and W. Takeuchi, "Quantitative assessment and driving force analysis of mangrove forest changes in China from 1985 to 2018 by integrating optical and radar imagery," *Int. Soc. Photogrammetry Remote Sens. Int. J. Geo-Inf.*, vol. 9, no. 9, p. 513, 2020.

[17] M. J. C. Buitre, H. Zhang, and H. Lin, "The mangrove forests change and impacts from tropical cyclones in the Philippines using time series satellite imagery," *Remote Sens.*, vol. 11, no. 6, p. 688, 2019.

[18] T. D. Pham, D. T. Bui, K. Yoshino, and N. N. Le, "Optimized rule-based logistic model tree algorithm for mapping mangrove species using ALOS PALSAR imagery and GIS in the tropical region," *Environ. Earth Sci.*, vol. 77, no. 5, p. 159, 2018.

[19] J. Xia, N. Yokoya, and T. D. Pham, "Probabilistic mangrove species mapping with multiple-source remote-sensing datasets using label distribution learning in Xuan Thuy National Park, Vietnam," *Remote Sens.*, vol. 12, no. 22, 2020, Art. no. 3834.

[20] H. Ren et al., "Wetland changes and mangrove restoration planning in Shenzhen Bay, Southern China," *Landscape Ecological Eng.*, vol. 7, pp. 241–250, 2011.

[21] M. Wang, W. Cao, Q. Guan, G. Wu, and F. Wang, "Assessing changes of mangrove forest in a coastal region of southeast China using multi-temporal satellite images," *Estuarine, Coastal Shelf Sci.*, vol. 207, pp. 283–292, 2018.

[22] T. Wang, H. Zhang, H. Lin, and C. Fang, "Textural–spectral feature-based species classification of mangroves in Mai Po nature reserve from Worldview-3 imagery," *Remote Sens.*, vol. 8, no. 1, p. 24, 2015.

[23] M. Jia et al., "Mapping China's mangroves based on an object-oriented classification of Landsat imagery," *Wetlands*, vol. 34, pp. 277–283, 2014.

[24] M. Jia, Z. Wang, Y. Zhang, D. Mao, and C. Wang, "Monitoring loss and recovery of mangrove forests during 42 years: The achievements of mangrove conservation in China," *Int. J. Appl. Earth Observ. Geoinf.*, vol. 73, pp. 535–545, 2018.

[25] C. Lu et al., "Dynamic analysis of mangrove forests based on an optimal segmentation scale model and multi-seasonal images in Quanzhou Bay, China," *Remote Sens.*, vol. 10, no. 12, 2018, Art. no. 2020.

[26] L. Hu, W. Li, and B. Xu, "Monitoring mangrove forest change in China from 1990 to 2015 using Landsat-derived spectral-temporal variability metrics," *Int. J. Appl. Earth Observ. Geoinf.*, vol. 73, pp. 88–98, 2018.

[27] K. F. Peng, "Remote sensing classification of wetlands in coastal urban agglomerations and simulation of future spatial changes: A case study of Guangdong-Hong Kong-Macao Greater Bay area and Guangxi Beibu Gulf," Ph.D. dissertation, Dept. Geographic Sci., Beijing Normal Univ., Beijing, China, 2022.

[28] T. Zhang et al., "A fine-scale mangrove map of China derived from 2-meter resolution satellite observations and field data," *Int. Soc. Photogrammetry Remote Sens. Int. J. Geo-Inf.*, vol. 10, no. 2, p. 92, 2021.

[29] J. Zhang, X. Yang, Z. Wang, T. Zhang, and X. Liu, "Remote sensing based spatial-temporal monitoring of the changes in coastline mangrove forests in China over the last 40 years," *Remote Sens.*, vol. 13, no. 10, 2021, Art. no. 1986.

[30] C.-P. Zhao and C.-Z. Qin, *A Detailed Mangrove Map of China for 2019 Derived from Sentinel-1 and-2 Images and Google Earth Images*. Hoboken, NJ, USA: Wiley, 2022.

[31] P. Wu, J. Zhang, Y. Ma, and X. Li, "Remote sensing monitoring and analysis of the changes of mangrove resources in China in the past 20 years," *Adv. Mar. Sci.*, vol. 31, pp. 406–414, 2013.

[32] B. W. Liao and Q. M. Zhang, "Area, distribution and species composition of mangroves in China," *Wetland Sci.*, vol. 12, no. 4, pp. 435–440, 2014.

[33] Z. Zhang, N. Xu, Y. Li, and Y. Li, "Sub-continental-scale mapping of tidal wetland composition for East Asia: A novel algorithm integrating satellite tide-level and phenological features," *Remote Sens. Environ.*, vol. 269, 2022, Art. no. 112799.

[34] J. Wang et al., "Consistency analysis and accuracy assessment of three global ten-meter land cover products in rocky desertification region—A case study of southwest China," *Int. Soc. Photogrammetry Remote Sens. Int. J. Geo-Inf.*, vol. 11, no. 3, p. 202, 2022.

[35] P. Liu, J. Pei, H. Guo, H. Tian, H. Fang, and L. Wang, "Evaluating the accuracy and spatial agreement of five global land cover datasets in the ecologically vulnerable south China Karst," *Remote Sens.*, vol. 14, no. 13, 2022, Art. no. 3090.

[36] Y. Yang, P. Xiao, X. Feng, and H. Li, "Accuracy assessment of seven global land cover datasets over China," *Int. Soc. Photogrammetry Remote Sens. J. Photogrammetry Remote Sens.*, vol. 125, pp. 156–173, 2017.

[37] L. Liang, Q. Liu, G. Liu, H. Li, and C. Huang, "Accuracy evaluation and consistency analysis of four global land cover products in the Arctic region," *Remote Sens.*, vol. 11, no. 12, 2019, Art. no. 1396.

[38] T. Hua, W. Zhao, Y. Liu, S. Wang, and S. Yang, "Spatial consistency assessments for global land-cover datasets: A comparison among GLC2000, CCI LC, MCD12, GLOBCOVER and GLCNMO," *Remote Sens.*, vol. 10, no. 11, 2018, Art. no. 1846.

[39] Y. Bai, M. Feng, H. Jiang, J. Wang, Y. Zhu, and Y. Liu, "Assessing consistency of five global land cover data sets in China," *Remote Sens.*, vol. 6, no. 9, pp. 8739–8759, 2014.

[40] Z. S. Venter, D. N. Barton, T. Chakraborty, T. Simensen, and G. Singh, "Global 10 m land use land cover datasets: A comparison of dynamic world, world cover and Esri land cover," *Remote Sens.*, vol. 14, no. 16, 2022, Art. no. 4101.

[41] X. Chen, L. I. N. Ya, M. Zhang, Y. U. Le, H. LI, and Y. BAI, "Assessment of the cropland classifications in four global land cover datasets: A case study of Shaanxi Province, China," *J. Integrative Agriculture*, vol. 16, no. 2, pp. 298–311, 2017.

[42] K. Jia, S. S. Chen, and W. G. Jiang, "Long time-series remote sensing monitoring of mangrove forests in the Guangdong-Hong Kong-Macao Greater Bay area," *Nat. Remote Sens. Bull.*, vol. 26, pp. 1096–1111, 2022.

[43] Z. Zhang, W. Jiang, K. Peng, Z. Wu, Z. Ling, and Z. Li, "Assessment of the impact of wetland changes on carbon storage in coastal urban agglomerations from 1990 to 2035 in support of SDG15. 1," *Sci. Total Environ.*, vol. 877, 2023, Art. no. 162824.

[44] Y. Lingyun, L. Shenhui, J. Xueyao, S. Xiaoxue, and L. Ruili, "Ecological problems and protection countermeasures of mangrove wetland in Guangdong-Hong Kong-Macao Greater Bay area," *Acta Sci. Nat. Univ. Pekinensis*, vol. 55, no. 4, pp. 782–790, 2019.

[45] H.-Z. Zhou et al., "Distribution fractions and potential ecological risk assessment of heavy metals in mangrove sediments of the Greater Bay area," *Environ. Sci. Pollut. Res.*, vol. 30, no. 16, pp. 45859–45871, 2023.

[46] L. Wang, M. Jia, D. Yin, and J. Tian, "A review of remote sensing for mangrove forests: 1956–2018," *Remote Sens. Environ.*, vol. 231, 2019, Art. no. 111223.

[47] R. L. Morris, B. Fest, D. Stokes, C. Jenkins, and S. E. Swearer, "The coastal protection and blue carbon benefits of hybrid mangrove living shorelines," *J. Environ. Manage.*, vol. 331, 2023, Art. no. 117310.

[48] A. Comber, P. Fisher, C. Brunsdon, and A. Khmag, "Spatial analysis of remote sensing image classification accuracy," *Remote Sens. Environ.*, vol. 127, pp. 237–246, 2012.

[49] D. M. Alongi, "Carbon cycling and storage in mangrove forests," *Annu. Rev. Mar. Sci.*, vol. 6, pp. 195–219, 2014.

[50] Z. Zhu, C. E. Woodcock, and P. Olofsson, "Continuous monitoring of forest disturbance using all available Landsat imagery," *Remote Sens. Environ.*, vol. 122, pp. 75–91, 2012.

[51] M. J. McCarthy, K. R. Radabaugh, R. P. Moyer, and F. E. Muller-Karger, "Enabling efficient, large-scale high-spatial resolution wetland mapping using satellites," *Remote Sens. Environ.*, vol. 208, pp. 189–201, 2018.

[52] C. Zhao and C.-Z. Qin, "10-m-resolution mangrove maps of China derived from multi-source and multi-temporal satellite observations," *Int. Soc. Photogrammetry Remote Sens. J. Photogrammetry Remote Sens.*, vol. 169, pp. 389–405, 2020.

[53] Q. Xia, C.-Z. Qin, H. Li, C. Huang, and F.-Z. Su, "Mapping mangrove forests based on multi-tidal high-resolution satellite imagery," *Remote Sens.*, vol. 10, no. 9, 2018, Art. no. 1343.

[54] K. Rogers, L. Lymburner, R. Salum, B. P. Brooke, and C. D. Woodroffe, "Mapping of mangrove extent and zonation using high and low tide composites of Landsat data," *Hydrobiologia*, vol. 803, pp. 49–68, 2017.

[55] D. S. Collins et al., "Tidal dynamics and mangrove carbon sequestration during the Oligo–Miocene in the South China Sea," *Nature Commun.*, vol. 8, no. 1, 2017, Art. no. 15698.

[56] C. Giri, Z. Zhu, L. L. Tieszen, A. Singh, S. Gillette, and J. A. Kelmelis, "Mangrove forest distributions and dynamics (1975–2005) of the tsunami-affected region of Asia," *J. Biogeography*, vol. 35, no. 3, pp. 519–528, 2008.

[57] A. Verhegghen et al., "The potential of Sentinel satellites for burnt area mapping and monitoring in the Congo Basin forests," *Remote Sens.*, vol. 8, no. 12, p. 986, 2016.

[58] B. Chen et al., "A mangrove forest map of China in 2015: Analysis of time series Landsat 7/8 and Sentinel-1A imagery in Google Earth Engine cloud computing platform," *Int. Soc. Photogrammetry Remote Sens. J. Photogrammetry Remote Sens.*, vol. 131, pp. 104–120, 2017.

[59] N. Gorelick, M. Hancher, M. Dixon, S. Ilyushchenko, D. Thau, and R. Moore, "Google Earth Engine: Planetary-scale geospatial analysis for everyone," *Remote Sens. Environ.*, vol. 202, pp. 18–27, 2017.

[60] X. Zhang et al., "GWL_FCS30: Global 30 m wetland map with fine classification system using multi-sourced and time-series remote sensing imagery in 2020," *Earth Syst. Sci. Data Discuss.*, vol. 2022, pp. 1–31, 2022.

[61] B. Fu et al., "Quantifying scattering characteristics of mangrove species from Optuna-based optimal machine learning classification using multi-scale feature selection and SAR image time series," *Int. J. Appl. Earth Observ. Geoinformation*, vol. 122, 2023, Art. no. 103446.

[62] J. Zheng, H. Wei, R. Chen, J. Liu, L. Wang, and W. Gu, "Invasive trends of Spartina Alterniflora in the southeastern Coast of China and potential distributional impacts on mangrove forests," *Plants*, vol. 12, no. 10, 2023, Art. no. 1923.

Ziyan Ling received the B.S. degree in geographic information system from Nanjing Forestry University, Nanjing, China, in 2008, and the M.S. degree in cartography and geographical information system in 2011 from Beijing Normal University, Beijing, China, where she is currently working toward the Ph.D. degree in cartography and GIS.

She is currently a 3S Teaching and Scientific Research with Nanning Normal University, Nanning, China.

Zhijie Xiao received the B.S. degree in geographic information science from Southwest Jiaotong University, Chengdu, China, in 2022. He is currently working toward the master's degree in cartography and geographical information system with Beijing Normal University, Beijing, China.

His research interests include mangrove mapping and remote sensing of wetlands.
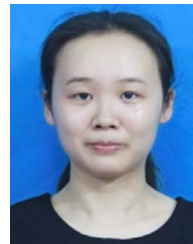
Yawen Deng received the B.S. degree in geographic information science from Beijing Normal University, Beijing, China, in 2020, and the M.S. degree in cartography and geographical information engineering from Beijing Normal University, Beijing, China, in 2023.

Her research interests include surface water mapping and remote sensing of wetlands.

Weiguo Jiang received the B.S. degree in geography from Hunan Normal University, Changsha, China, in 1999, the M.S. degree in physical geography from Nanjing Normal University, Nanjing, China, in 2003, and the Ph.D. degree in cartography and geographic Information System from Beijing Normal University, Beijing, China, in 2006.

He is currently a Professor with Beijing Normal University. His research interests include remote sensing, hydrology and international urban wetland protection, and exploration of SDGs.

Ze Zhang received the M.S. degree in cartography and geographic information systems from Nanning Normal University, Nanning, China, in 2022. He is currently working toward the Ph.D. degree in cartography and geographical information system with Beijing Normal University, Beijing, China.

His research interests include wetland remote sensing extraction, wetland spatial intelligent simulation, and comprehensive evaluation.

Zhifeng Wu received the B.S. degree in geography education from Hunan Normal University, Changsha, China, in 1992, the M.S. degree in physical geography from South China Normal University, Guangzhou, China, in 1995, and the Ph.D. degree in geographic information science from the Institute of Geographical Sciences and Natural Resources, Chinese Academy of Sciences, Beijing, China, in 2002.

He is currently a Professor with the School of Geographical Sciences and Remote Sensing, Guangzhou University, Guangzhou, China. His research interests include urban remote sensing, land ecological remote sensing, spatiotemporal data analysis, and monitoring and assessment of natural resources.

Kaifeng Peng received the M.S. degree in surveying and mapping engineering from Wuhan University, Wuhan, China, in 2017, and the Ph.D. degree in remote sensing and GIS from Beijing Normal University, Beijing, China, in 2022.

He is currently a Lecturer with Tianjin Normal University, Tianjin, China. His research interests include wetland classification, land use simulation, and ecological evaluation.